Chinese Journal of Natural Medicines

A CYP80B enzyme from *Stephania tetrandra* enables the 3'–hydroxylation of *N*–methylcoclaurine and coclaurine in the biosynthesis of benzylisoquinoline alkaloids

Yaoting Li, Yuhan Feng, Wan Guo, Yu Gao, Jiatao Zhang, Lu Yang, Chun Lei, Yun Kang, Yaqin Wang, Xudong Qu, Jianming Huang

Citation: Yaoting Li, Yuhan Feng, Wan Guo, Yu Gao, Jiatao Zhang, Lu Yang, Chun Lei, Yun Kang, Yaqin Wang, Xudong Qu, Jianming Huang, A CYP80B enzyme from *Stephania tetrandra* enables the 3'–hydroxylation of *N*–methylcoclaurine and coclaurine in the biosynthesis of benzylisoquinoline alkaloids, Chinese Journal of Natural Medicines, 2025, 23(5), 630–640. doi: 10.1016/S1875–5364(25)60867–3.

View online: https://doi.org/10.1016/S1875–5364(25)60867–3

Chinese Journal of Natural Medicines 23 (2025) 630-640

Contents lists available at ScienceDirect

Chinese Journal of Natural Medicines

journal homepage: www.cjnmcpu.com/

Original article

A CYP80B enzyme from *Stephania tetrandra* enables the 3'-hydroxylation of *N*-methylcoclaurine and coclaurine in the biosynthesis of benzylisoquinoline alkaloids

Yaoting Li[a,b,Δ], Yuhan Feng[a,Δ], Wan Guo[a], Yu Gao[a,c], Jiatao Zhang[a], Lu Yang[b], Chun Lei[a], Yun Kang[a], Yaqin Wang[a], Xudong Qu[b,*], Jianming Huang[a,*]

[a] *School of Pharmacy, Fudan University, Shanghai 201203, China*
[b] *State Key Laboratory of Microbial Metabolism and School of Life Sciences and Biotechnology, Shanghai Jiao Tong University, Shanghai 200240, China*
[c] *School of Pharmacy, East China University of Science and Technology, Shanghai 200237, China*

ARTICLE INFO

Article history:
Received 2 October 2024
Revised 30 November 2024
Accepted 22 December 2024
Available online 20 May 2025

Keywords:
Stephania tetrandra
Cytochrome P450
CYP80B
CYP450 reductase
Benzylisoquinoline alkaloid

ABSTRACT

Benzylisoquinoline alkaloids (BIAs) are a structurally diverse group of plant metabolites renowned for their pharmacological properties. However, sustainable sources for these compounds remain limited. Consequently, researchers are focusing on elucidating BIA biosynthetic pathways and genes to explore alternative sources using synthetic biology approaches. CYP80B, a family of cytochrome P450 (CYP450) enzymes, plays a crucial role in BIA biosynthesis. Previously reported CYP80Bs are known to catalyze the 3′-hydroxylation of (*S*)-*N*-methylcoclaurine, with the *N*-methyl group essential for catalytic activity. In this study, we successfully cloned a full-length CYP80B gene (*StCYP80B*) from *Stephania tetrandra* (*S. tetrandra*) and identified its function using a yeast heterologous expression system. Both *in vivo* yeast feeding and *in vitro* enzyme analysis demonstrated that *St*CYP80B could catalyze *N*-methylcoclaurine and coclaurine into their respective 3′-hydroxylated products. Notably, *St*CYP80B exhibited an expanded substrate selectivity compared to previously reported wild-type CYP80Bs, as it did not require an *N*-methyl group for hydroxylase activity. Furthermore, *St*CYP80B displayed a clear preference for the (*S*)-configuration. Co-expression of *St*CYP80B with the CYP450 reductases (CPRs, *St*CPR1, and *St*CPR2), also cloned from *S. tetrandra*, significantly enhanced the catalytic activity towards (*S*)-coclaurine. Site-directed mutagenesis of *St*CYP80B revealed that the residue H205 is crucial for coclaurine catalysis. Additionally, *St*CYP80B exhibited tissue-specific expression in plants. This study provides new genetic resources for the biosynthesis of BIAs and further elucidates their synthetic pathway in natural plant systems.

1. Introduction

Benzylisoquinoline alkaloids (BIAs) constitute a class of plant metabolites predominantly found in the Ranunculales order, particularly in the Ranunculaceae, Papaveraceae, Menispermaceae, Berberidaceae, and Magnoliaceae families. These natural alkaloids exhibit remarkable structural diversity, encompassing multiple subclasses, including monobenzylisoquinoline, bisbenzylisoquinoline, protobeberine, aporphine, and morphinan. Medicinal plants containing BIAs have been integral to traditional pharmaceutical practices, notably in China. To date, numerous BIAs have gained approval as analgesics, antitussives, muscle relaxants, neuromuscular blockers, and smooth muscle relaxants. Furthermore, research has demonstrated their potential in addressing viral infections, cancer, malaria, HIV, and psychosis [1, 2].

The production of BIAs presents challenges due to limited natural sources and high chemical synthesis costs, impeding the development of BIA-based pharmaceuticals. Synthetic biology offers a promising solution to this issue. Consequently, researchers are focusing on elucidating the natural BIA biosynthetic pathway and establishing microbial systems for BIA production [3]. As depicted in Fig. 1, the complex BIA biosynthesis process begins with the conversion of L-tyrosine into dopamine and 4-hydroxyphenylacetaldehyde. These compounds subsequently undergo a subsequent condensation to form (*S*)-norcoclaurine, catalyzed by (*S*)-norcoclaurine synthase (NCS) [4]. Following the 6-*O*-methylation that transforms (*S*)-norcoclaurine into (*S*)-coclaurine [5], two distinct natural biosynthetic pathways have been proposed. One proceeds through *N*-methylation to form (*S*)-*N*-methylcoclaurine, followed by several *N*-methylated intermediates, including (*S*)-reticuline —a crucial precursor for most BIA subclasses (the *N*-methylated pathway in Fig. 1) [5, 6]. The other pathway involves a series of *N*-desmethylated intermediates, converting (*S*)-coclaurine into (*S*)-3′-hydroxy-coclaurine and (*S*)-norreticuline sequen-

* Corresponding author.
E-mail addresses: quxd19@sjtu.edu.cn (X. Qu); jmhuang@shmu.edu.cn (J. Huang)
Δ These authors contributed equally to this work.

https://doi.org/10.1016/S1875-5364(25)60867-3

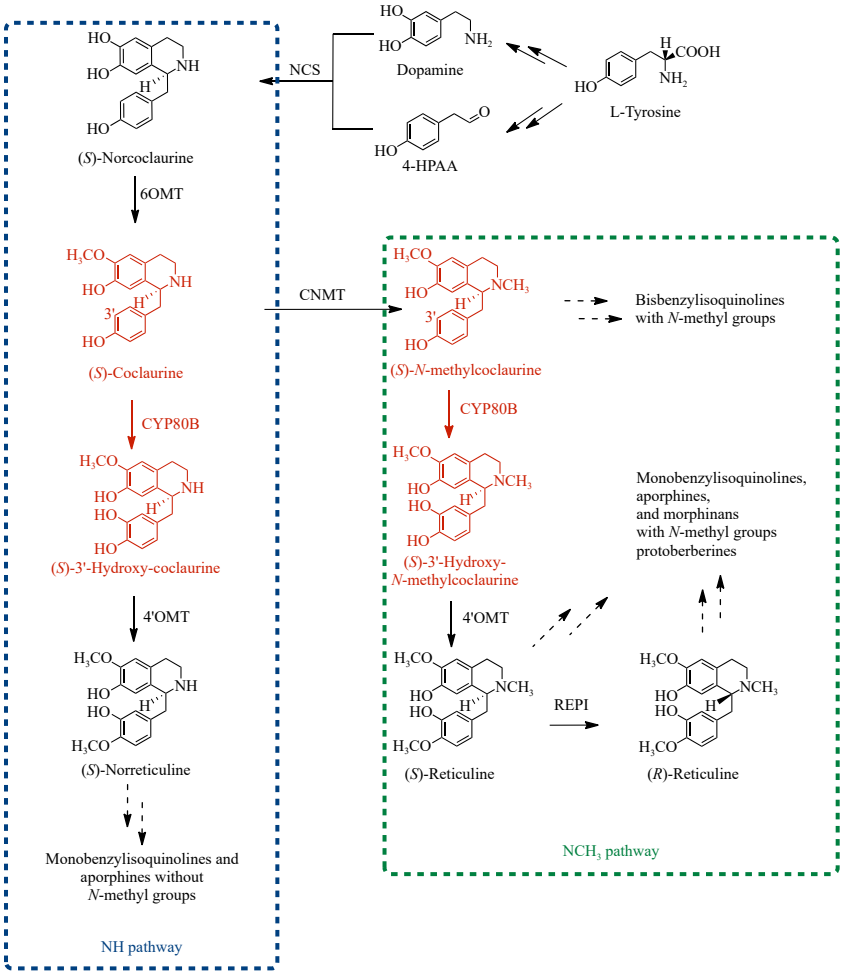

Fig. 1 Proposed biosynthetic pathways for benzylisoquinoline alkaloids (BIAs). Hydroxylation reactions identified in this study are highlighted in red. The dotted arrows indicate multiple enzymes and conversion steps. Blue dashed and green dashed boxes indicate *N*-desmethylated (the NH pathway) and *N*-methylated (the NCH_3 pathway) pathways, respectively.

tially [7] (the *N*-desmethylated pathway in Fig. 1). The former pathway is well-established and extensively documented in existing literature, with the associated enzymes having been successfully identified [3-11]. In contrast, the latter pathway is mentioned in only a few articles, possibly due to incomplete enzyme characterization [7, 11]. Notably, a key enzyme responsible for the hydroxylation of (*S*)-coclaurine to (*S*)-3'-hydroxy-coclaurine remains unidentified.

In the natural *N*-desmethylated pathway, enzymes from the CYP80 family of cytochrome P450 (CYP450) are responsible for the 3' position hydroxylation of BIAs. These enzymes, identified as CYP80Bs, are also known as *N*-methylcoclaurine hydroxylases (NMCH) due to their role in catalyzing the 3'-hydroxylation of (*S*)-*N*-methylcoclaurine. This has been observed in several plant species (Fig. 1), including *Eschscholzia californica* (*Ec*CYP80B) [8], *Papaver somniferum* (*Ps*CYP80B) [9], and *Corydalis yanhusuo* (*Cy*CYP80B) [10].CYP80Bs exhibit high substrate specificity, requiring an *N*-methyl group in the substrate for hydroxylase activity. Experimental evidence confirms that *Ec*CYP80B and *Cy*CYP80B do not exhibit hydroxylation effects on coclaurine, an *N*-demethylated substrate [8, 10]. While a recent study developed an *Ec*CYP80B variant displaying activity on coclaurine [11], the capacity of wild-type CYP80Bs to catalyze hydroxylation on *N*-demethylated BIAs remains uncertain.

Stephania tetrandra S. Moore (Menispermaceae) is a renowned traditional Chinese medicinal plant with a history spanning millennia. The *Chinese Pharmacopoeia* documents the extensive use of its roots for treating arthritis, rheumatism, edema, and eczema [12]. The primary bioactive components of this species are BIAs, comprising various subtypes. Phytochemical studies have revealed that *S. tetrandra* contains BIAs both without *N*-methyl groups (such as coclaurine and norreticuline) and with *N*-methyl groups (including *N*-methylcoclaurine and reticuline) [13-16]. Our preliminary liquid chromatography-tandem mass spectrometry (LC-MS/MS) analysis identified the presence of coclaurine, 3'-hydroxy-coclaurine, *N*-methylcoclaurine, and its corresponding 3'-hydroxylation derivative in the roots of *S. tetrandra* (Supplementary Fig. S1). This finding highlights the potential of *S. tetrandra* as an ideal candidate species for discovering a wild-type CYP80B enzyme capable of hydroxylating *N*-demethylated BIAs.

This study successfully cloned a full-length CYP80B gene from *S. tetrandra* (successfully cloned a full-length *CYP80B* gene (*StCYP80B*)) and elucidated its function using a yeast heterologous expression system. Notably, *St*CYP80B demonstrated hydroxylation activity on both (*S*)-coclaurine and (*S*)-*N*-methylcoclaurine, indicating an expanded substrate selectivity compared to the previously reported wild-type CYP80Bs. The research further examined the stereoselectivity of *St*CYP80B, the influence of CYP450 reductases (CPRs) from *S. tetrandra* (*St*CPR1 and *St*CPR2) on its catalytic activity, and identified key amino acids crucial for coclaurine catalysis. Moreover, the study investigated the expression patterns of *StCYP80B* and *CPR sequences from S. tetrandra* (*StCPRs*) in plant tissues. The identification of *St*CYP80B contributes new genetic elements for BIA biosynthesis, supporting the proposed *N*-desmethylated pathway in nat-

ural plant systems.

2. Material and methods

2.1. Plant materials and chemicals

S. tetrandra specimens were obtained from Yichun City, Jiangxi Province, China, in May 2019 and verified by Dr. Y. Kang at the School of Pharmacy, Fudan University. Fresh plant samples intended for ribonucleic acid (RNA) extraction were cleaned, sectioned appropriately, and immediately submerged in RNA-Be-Locker A solution provided by Sangon Biotech (Shanghai, China) for transport. Long-term storage is maintained at a temperature of −80 °C.

(±)-coclaurine and (±)-norcoclaurine were acquired from Weikeqi Biotech (Chengdu, China). (*R*)-*N*-methylcoclaurine and (±)-armepavine were procured from Desite Bio-Technology (Chengdu, China). (*S*)-3'-hydroxy-coclaurine and (*S*)-3'-hydroxy-*N*-methylcoclaurine were obtained from Toronto Research Chemicals (Mississauga, Canada). The stated purities of these chemicals exceeded 95%. *R*- and *S*-coclaurine were isolated from the purchased (±)-coclaurine *via* chiral HPLC, with their configurations confirmed through optical rotation data (refer to Supporting Information) [17, 18]. (±)-*N*-methylcoclaurine was synthesized from (±)-coclaurine utilizing a coclaurine *N*-methyltransferase (CNMT) as previously described [19], and its structure was verified by NMR and MS data (Supporting Information) [20].

2.2. Sequence analysis of candidate genes

The previously reported *S. tetrandra* transcriptome data [21] served as the foundation for identifying potential candidate sequences encoding CYP80Bs and CPRs. Building upon the earlier functional annotation results, candidate genes underwent further screening through blastp searches. Clustal Omega [22] was employed to align the deduced amino acid sequences of *St*CYP80B and *St*CPRs with known sequences. ESPript 3.0 [23] facilitated the generation of multiple alignment figures for the candidate genes. The complete nucleotide sequences of the candidate genes are accessible in Supplementary Table S1.

2.3. Phylogenetic analysis

Phylogenetic analysis was conducted using MEGA 7.0 software, employing the Neighbor-joining (NJ) method. The evolutionary distance was computed using the Poisson correction method. Bootstrap values, indicated on the branches, were assessed with 1000 replicates.

2.4. RNA isolation and gene cloning

RNA extraction from *S. tetrandra* was performed using the Omega Plant RNA Kit (Omega Bio-tek, USA). The extracted RNA was then reverse transcribed utilizing the Hifair® II 1st Strand complementary deoxyribonucleic acid (cDNA) Synthesis Kit (Yeasen Biotech, China). Full-length cDNAs of *StCYP80B* and *StCPRs* were amplified through polymerase chain reaction (PCR) using PrimeSTAR MAX DNA Polymerase (Takara, Japan) with the primers listed in Supplementary Table S2. All primers were designed using Primer Premier 5.0 software.

2.5. Construction of the yeast expression vector

Full-length cDNAs with homologous arms were amplified using the primers listed in Supplementary Table S3. *StCYP80B* and *StCPRs* were cloned into separate multiple cloning sites (MCS) sites regulated by the GAL1-GAL10 divergent promoter. Initially, *StCYP80B* was subcloned into the SacI/NotI-digested eukaryotic expression vector pESC-Leu (Invitrogen, USA) using the Multi One Step Cloning Kit (Yeasen Biotech, China). Subsequently, *StCPR1/2* cDNA was introduced into the XhoI/NheI-digested pESC-Leu-*StCYP80B* vector, resulting in the construction of recombinant plasmids pESC-Leu-*StCPR1-StCYP80B*, and pESC-Leu-*StCPR2-StCYP80B*. The recombinant plasmids were introduced into *Escherichia coli* DH5α (Yeasen Biotech, China). Positive clones were confirmed through bacterial PCR and DNA sequencing of extracted plasmids. The recombinant plasmids were then extracted using SanPrep Column Plasmid Mini-Prep Kits (Sangon Biotech, China).

2.6. Heterologous expression of candidate genes in yeast

The recombinant plasmids containing candidate genes (pESC-Leu-*StCYP80B*, pESC-Leu-*StCPR*1-*StCYP80B* and pESC-Leu-*StCPR2-StCYP80B*) were introduced into yeast (*Saccharomyces cerevisiae*) YPH499 utilizing the Frozen-EZ Yeast Transformation II kit (Zymo Research, USA) for heterologous expression. The YPH499 strain transformed with the empty vector pESC-Leu served as a control. The transformants were cultivated on a solid SD-Leu medium at 30 °C for 2–4 days. Positive transformants, verified through colony PCR, were subsequently cultured in a liquid SD-Leu medium (2% glucose) at 30 °C and 220 r·min^{-1} until reaching an OD_{600} of 0.8–1.2. The yeast cells were then transferred to an SG-Leu medium (containing 0.8 mmol·L^{-1} 5-aminolevulinic acid hydrochloride, 1.6 mmol·L^{-1}$FeSO_4$, and 2% galactose) to induce protein expression at 30 °C for 18–20 h. Finally, the yeast cells were then harvested by centrifugation (5000 r·min^{-1}, 10 min, 5 °C).

2.7. In vivo supplementary assay of recombinant yeast

After galactose induction, the recombinant yeast cells were resuspended in a buffer containing 50 mmol·L^{-1} phosphate-buffered saline (PBS, pH 7.4). Substrates were added to the suspension to achieve a final concentration of 0.06 mmol·L^{-1}. The catalysis process was conducted for 24 h at 30 °C with agitation at 220 r·min^{-1}, after which the reaction was terminated by the addition of an equal volume of methanol. The reaction samples were subjected to ultrasonic extraction for 15 min, followed by centrifugation at 5000 r·min^{-1} and 5 °C for 10 min. The resulting supernatant was then appropriately diluted with methanol and 0.05% aqueous formic acid in a 1 : 1 ratio (*V : V*) in preparation for LC-MS/MS analysis.

2.8. Extraction of yeast microsomal fractions and in vitro enzyme activity assays

Yeast microsomal fractions were prepared following a previously described method [24] with minor modifications. The yeast cells, collected as outlined in the *in vivo* supplementary assay section for recombinant yeast, were washed in buffer I (100 mmol·L^{-1} KCl, 50 mmol·L^{-1} Tris, 1 mmol·L^{-1} ethylene diamine tetraacetic acid (EDTA), pH 7.5) and subsequently resuspended in buffer II (20 mmol·L^{-1} β-mercaptoethanol, 1% BSA, 0.6 mol·L^{-1} sorbitol, 50 mmol·L^{-1} Tris, 1 mmol·L^{-1} EDTA, pH 7.5). An OMNI Bead Mill homogenizer was utilized to disrupt the yeast cells. The resulting lysate underwent centrifugation at 10 000 × g for 20 min to remove cell debris, followed by ultracentrifugation of the supernatant at 100 000 × g for 1 h to obtain the microsomal fraction. The microsomes were suspended in buffer III (30% Glycerin, 50 mmol·L^{-1} Tris, 1 mmol·L^{-1} EDTA). Protein concentration was determined using the Modified Bradford Protein Assay Kit (Sagon Biotech, Shanghai, China), with bovine serum albumin serving as the standard.

The *in-vitro* activity was evaluated in a 500 μL reaction system, comprising 0.005 mmol·L^{-1} flavin adenine dinucleotide (FAD), 0.005 mmol·L^{-1} flavin mononucleotide (FMN), 1 mmol·L^{-1} NADP^{+},20 mmol·L^{-1} glucose, 1 unit of glucose-6-phosphate dehydrogenase, 0.1 mmol·L^{-1} substrate, and approximately 400 μg of microsomal protein. Following incubation at 30 °C and 220 r·min^{-1} for 2 h, the reactions were terminated by the addition of an equal volume of methanol. The reaction samples were subsequently diluted appropriately with methanol and 0.05% aqueous formic acid in a 1 : 1 ratio (*V : V*) for LC-MS/MS analysis.

2.9. Protein modeling, molecular docking, and site-directed mutagenesis

Structural prediction of *St*CYP80B and the *St*CYP80B^{H205Y} mutant was conducted using AlphaFold 3.0 (https://www.alphafoldserver.com) [25]. Molecular docking of the predicted protein model and its substrates was executed using Discovery Studio 2019, with subsequent molecular graphics rendered using PyMOL 2.5.4 (http://www.pymol.org/).

Site-directed mutagenesis of the *StCYP80B* gene was performed using the PCR method with specific mutant primers. The resulting PCR product underwent DpnI digestion to eliminate the template plasmid. The digested product was then transformed into *E. coli* DH5α cells for amplification. The generated recombinant plasmids, including pESC-Leu-*StCYP80B*^{H205Y}, pESC-Leu-*StCPR1-StCYP80B*^{H205Y}, and pESC-Leu-*StCPR2-StCYP80B*^{H205Y}, were subsequently expressed and functionally characterized in yeast cells.

2.10. Expression analysis with quantitative real-time PCR (qRT-PCR)

To evaluate the expression levels of the *StCYP80B* and *StCPRs* in various tissues of *S. tetrandra*, qRT-PCR amplification was conducted using an ABI QuantStudio3 RT-PCR system (Thermo Fisher, USA). RNA extracted from different tissues underwent treatment with a DNA digester mix to eliminate DNA contamination, followed by cDNA synthesis using Hifair® Ⅲ supermix plus (Yeasen Biotech, China). The qRT-PCR experiment utilized the SYBR Green Master Mix (Yeasen Biotech, China) according to the manufacturer's protocol. The *S. tetrandra actin* gene served as an internal reference to normalize expression levels [21]. Gene-specific primers and internal reference gene primers (detailed in Supplementary Table S4) were designed using Primer Premier 5.0 software. The relative expression of each gene was determined using the $2^{-\triangle\triangle CT}$ method [26].

2.11. LC-MS/MS analysis

The sample analysis was performed using a UPLC-triple quadrupole (QqQ)-MS/MS system (Shimadzu, Japan) equipped with a Venusil XBP PH C_{18} column (2.1 mm × 100 mm, 5 μm, Agela Technologies, Tianjin, China). The mobile phase comprised a 0.1% formic acid aqueous solution (A) and acetonitrile (B), with a flow rate of 0.5 mL·min^{-1}. The elution program was as follows: 5%–25% B at 0–5 min, 25%–95% B at 5–7 min, 95% B at 7–9 min, 95%–5% B at 9–10 min, and 5% B at 10–13 min. The column temperature was maintained at 40 °C, and the injection volume was 2 μL.

The QqQ–MS/MS scan parameters were configured as follows: ESI interface; nebulizing gas flow at 3 L·min^{-1}; heating gas flow at 10 L·min^{-1}; interface temperature of 300 °C; DL temperature of 250 °C; heat block temperature of 400 °C; and drying gas flow at 10 L·min^{-1}. The MS/MS scan parameters, including precursor/product ion transition, Q1 pre-bias, collision energy, and Q3 pre-bias, were optimized for each analyte: *N*-methylcoclaurine (*m/z* 300.25/107.15, −26.0 V, −25.0 V, and −26.0 V); coclaurine (*m/z* 286.25/107.15, −22.0 V, −28.0 V, and −20.0 V); 3'-hydroxy-*N*-methylcoclaurine (*m/z* 316.15/123.05, −21.0 V, −27.0 V, and −12.0 V); and 3'-hydroxy-coclaurine (*m/z* 302.15/123.05, −21.0 V, −27.0 V, and −12.0 V). The dwell time was set at 100.0 msec for all the analytes.

3. Results and discussion

3.1. Sequences analyses of StCYP80B and StCPR

The potential candidate sequences of *CYP80B* and *CPR*, initially annotated based on the *S. tetrandra* transcriptome dataset in our previous study [21], underwent further screening through blastp homolog search. A full-length *CYP80B* sequence was successfully cloned from *S. tetrandra* and designated as *StCYP80B*. This sequence comprises 1473 nucleotides, encoding 491 amino acids. Multiple sequence alignments of amino acid sequences revealed that *St*CYP80B shared approximately 70% sequence identity with CYP80Bs from other species, including *Ec*CYP80B1 (68.17%) [8], *Cj*CYP80B2 (72.99%) [24], *Ps*CYP80B3 (74.53%) [9], *Tf*CYP80B4 (71.96%) [27], and *Cy*CYP80B (75.10%) [10]. Fig. 2 illustrates the amino acid sequences, secondary structure elements, and conserved regions of these CYP80Bs. Notably, highly conserved motifs were identified among the six CYP80B sequences, including the Helix-I region, the heme-binding region of Helix-L, the transmembrane helix followed by a short linker region consisting of approximately ten amino acids, and the proline-rich region.

CPRs function as essential partners for CYP450s in eukaryotes [28], prompting the screening of candidate CPR genes from the *S. tetrandra* transcriptome dataset using blastp homolog search. Previous research has demonstrated that CPR homologs in flowering plants exhibit high conservation, with sequence identities ranging from 65% to 80% [29]. Consistently, two candidate *StCPR*s displayed high similarity (sequence identities exceeding 65%) to previously identified *CPR*s from other species. Alignment of the deduced amino acid sequences of the *St*CPRs with the reported *CPR*s revealed five CPR-related conserved motifs were identified in all CPR proteins (as illustrated in Fig.3): the membrane anchor, FMN-, FAD-, P450-, and (reduced) nicotinamide adenine dinucleotide phosphate (NADPH)-binding domains.

CPRs from vascular plants can be categorized into two classes: Class I and Class II. Class I CPRs typically exhibit constitutive expression throughout plant growth and development, while Class II CPRs are inducible by injury or treatment with methyl jasmonate (MeJA)[29]. These two classes are distinguishable based on their N-terminal sequences preceding the hydrophobic region. Class I CPRs possess short *N*-terminal ends, whereas Class II CPRs have extended N-terminal ends with significant sequence identities[30]. Consequently, the two *StCPR*s are designated as *StCPR1* and *StCPR2*, with *StCPR1* presumed to belong to Class I and *StCPR2* to Class II based on their sequence characteristics.

3.2. Phylogenetic analyses of StCYP80B and StCPRs

The phylogenetic tree of CYP450s (Fig. 4A) was constructed using the deduced *St*CYP80B amino acid sequence, along with CYP80B homologs from other species, CYP450 hydroxylases involved in various metabolite biosynthetic processes, and other CYP450 genes associated with BIAs biosynthesis. In addition to CYP80B, other BIA-related CYP450s include CYP80A, CYP80G, CYP82, and CYP719, which catalyze C-O phenol-coupling, C-C phenol-coupling, hydroxylation, and methylenedioxy bridge formation, respectively[3, 24, 31-35]. The phylogenetic tree demon-

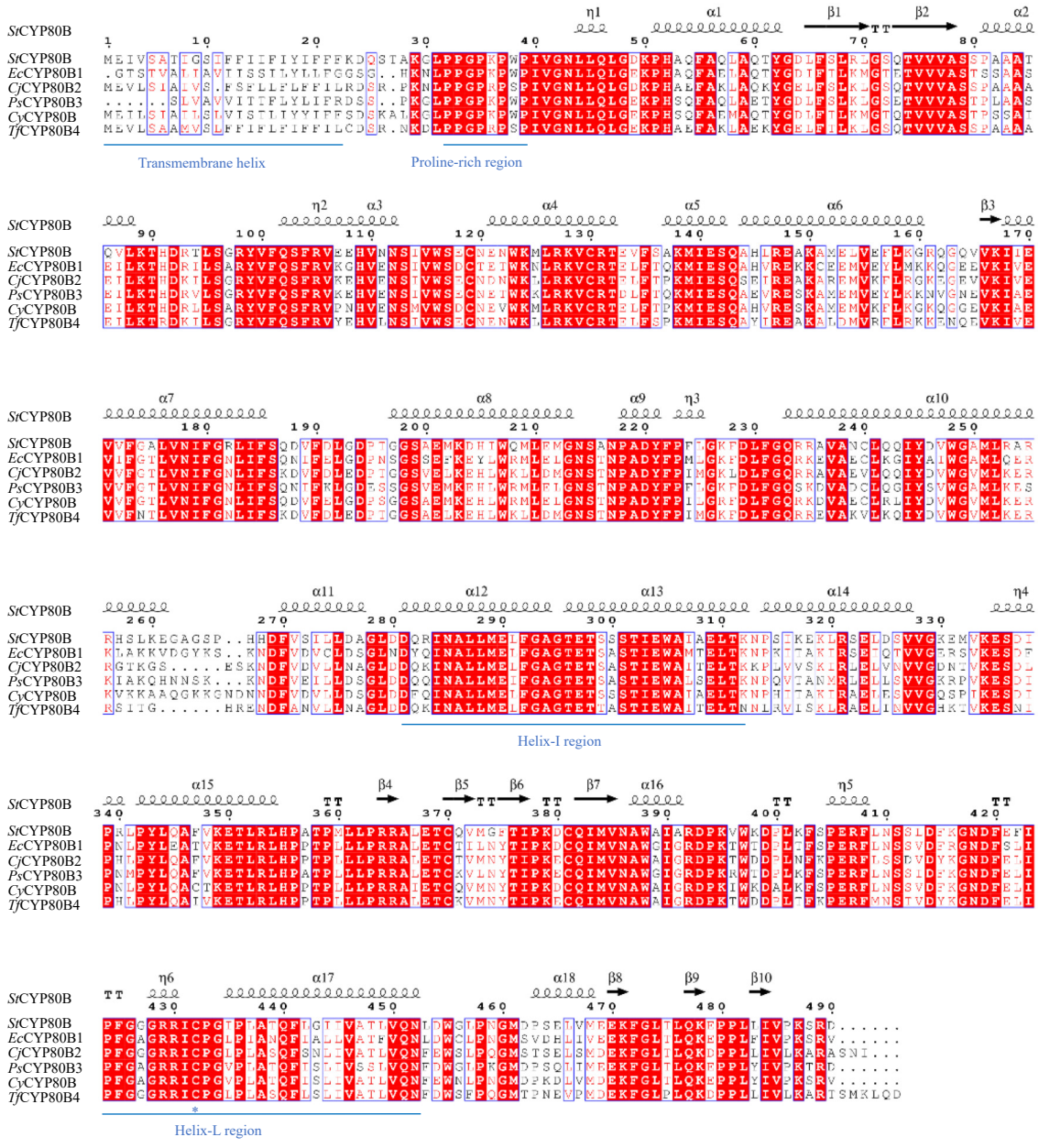

Fig. 2 Multiple alignments of amino acid sequences of CYP80Bs from *S. tetrandra* and other plants. The CYP80Bs from other species used are as follows: *Ec*CYP80B1 (*Eschscholzia californica*, AAC39452.1), *Cj*CYP80B2 (*Coptis japonica*, BAB12433.1), *Ps*CYP80B3 (*Papaver somniferum*, AAF61400.1), *Cy*CYP80B (*Corydalis yanhusuo*, No genbank id), and *Tf*CYP80B4 (*Thalictrum flavum subsp. glaucum*, AAU20767.1). For the secondary structure elements, helices are represented by squiggles, β-strands are depicted as arrows, and turns are indicated by "TT" letters.

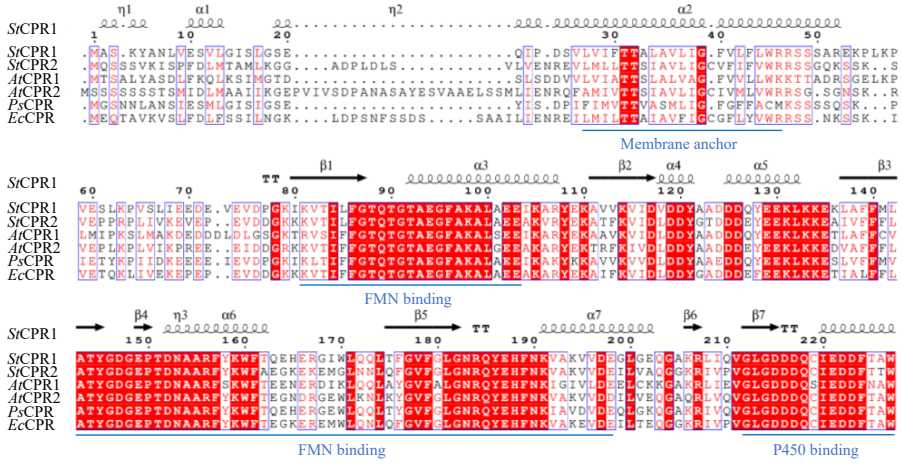

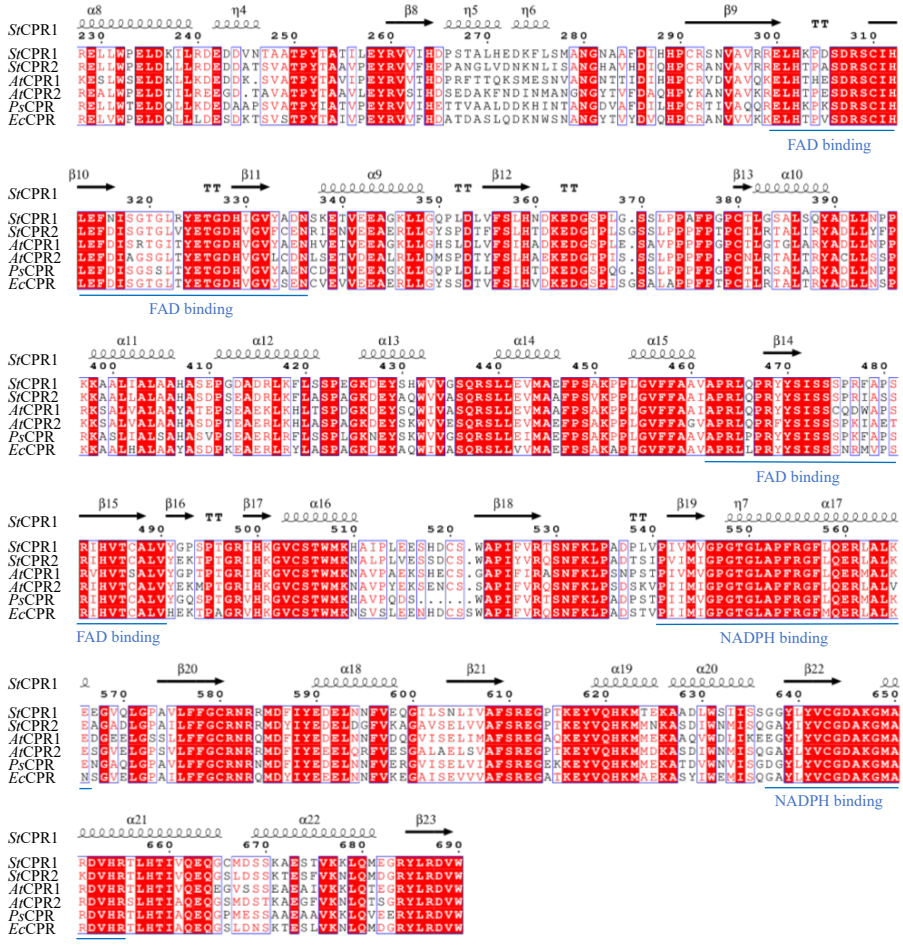

Fig. 3 Multiple alignment of amino acid sequences of CPRs from *S. tetrandra* and other plants. The CPRs from other species used are as follows: *At*CPR1 (*Arabidopsis thaliana*, CAA46814.1), *At*CPR2 (*Arabidopsis thaliana*, AAK17169.1), *Ps*CPR (*Papaver somniferum*, AAC05021.1), and *Ec*CPR (*Eschscholzia californica*, AAC05022.1). For the secondary structure elements, helices are represented by squiggles, β-strands are depicted as arrows, and turns are indicated by "TT" letters.

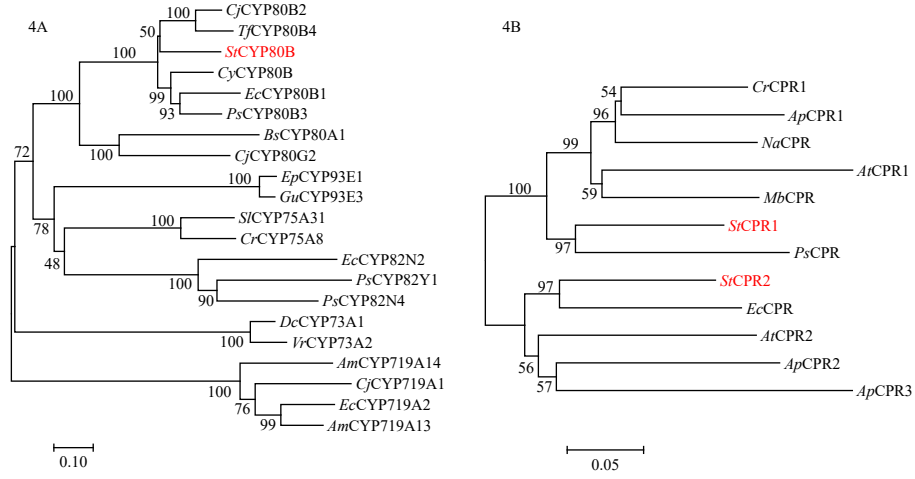

Fig. 4 Phylogenetic trees of CYP450s (4A) and CPRs (4B) from *S. tetrandra* and other plant species. The *St*CYP80B and *St*CPRs from *S. tetrandra* are marked in red. Bootstrap support values, calculated by 1000 replicates, are displayed on the branches. The reference genes are as follows: *Bs*CYP80A1(*Berberis stolonifera*, AAC48987.1), *Cj*CYP80G2 (*Coptis japonica*, BAF80448.1), *Ec*CYP80B1 (*Eschscholzia californica*, AAC39452.1), *Cj*CYP80B2 (*Coptis japonica*, BAB12433.1), *Ps*CYP80B3 (*Papaver somniferum*, AAF61400.1), *Tf*CYP80B4 (*Thalictrum flavum subsp. Glaucum*, AAU20767.1), *Cy*CYP80B (*Corydalis yanhusuo*, No genbank id), *Cj*CYP719A1 (*Coptis japonica*, BAB68769.1), *Ec*CYP719A2 (*Eschscholzia californica*, BAD98250.1), *Am*CYP719A13 (*Argemone mexicana*, ABR14721.1), *Am*CYP719A14 (*Argemone mexicana*, ABR14722.1), *Ps*CYP82Y1 (*Papaver somniferum*, I3PLR1.1), *Ec*CYP82N2 (*Eschscholzia californica*, F2Z9C1.1), *Ps*CYP82N4 (*Papaver somniferum*, L7X3S1.1), *Sl*CYP75A31 (*Solanum lycopersicum*, NP001234840.2), *Cr*CYP75A8 (*Catharanthus roseus*, Q9ZRY0), *Ep*CYP93E1 (*Entada phaseoloides*, UEP53726.1), *Gu*CYP93E3 (*Glycyrrhiza uralensis*, BAG68930.1), *Dc*CYP73A1 (*Dendrobium catenatum*, XP020701874.1), *Vr*CYP73A2 (*Vigna radiata*, NP001304077.1), *At*CPR1 (*Arabidopsis thaliana*, CAA46814.1), *At*CPR2 (*Arabidopsis thaliana*, AAK17169.1), *Ps*CPR (*Papaver somniferum*, AAC05021.1), *Ec*CPR (*Eschscholzia californica*, AAC05022.1), *Mb*CPR (*Mung bean*, A47298), *Na*CPR (*Nicotiana attenuate*, OIT38777.1), *Cr*CPR1 (*Catharanthus roseus*, AJA37723), *Ap*CPR1 (*Andrographis paniculate*, AQT38168.1), *Ap*CPR2 (*Andrographis paniculate*, AQT38169.1), and *Ap*CPR3 (*Andrographis paniculate*, AQT38170.1).

strates that the CYP450s cluster within specific families, such as the CYP80, CYP82, CYP93, CYP75, CYP73, and CYP719 clades. High bootstrap values associated with these clades indicate their reliable distinction within the established tree. Within the CYP80

clade, *St*CYP80B clusters together with CYP80B homologs from other species (*Ec*CYP80B1, *Cj*CYP80B2, *Ps*CYP80B3, *Tf*CYP80B4, and *Cy*CYP80B), all of which have been verified to catalyze the hydroxylation of (*S*)–*N*-methylcoclaurine at C-3′. CYP450 hydroxylases involved in other metabolite types, such as protoberberines (e.g., CYP82) [33], flavonoids (e.g., CYP75A) [36, 37], terpenoids (e.g., CYP93E) [38], and organic acids (e.g., CYP73A) [39, 40], exhibit a closer relationship to CYP80Bs than CYP719s, which catalyze methylenedioxy bridge formation in BIAs.

The phylogenetic tree of CPRs (Fig. 4B) was constructed using the deduced amino acid sequences of *St*CPRs, along with reported CPRs from other plant species. The analysis reveals that *St*CPR1 clusters with CPR Class I, which includes *At*CPR1 and *Ap*CPR1, while *St*CPR2 aligns with CPR Class II, encompassing *At*CPR2 and *Ap*CPR2 [41, 42]. Furthermore, *St*CPR1 and *St*CPR2 show close phylogenetic relationships with CPRs from Papaveraceae (*Ec*CPR and *Ps*CPR) [43], indicating their evolutionary proximity. These phylogenetic findings provide additional evidence supporting the classification and evolutionary relationships of *St*CPR1 and *St*CPR2.

3.3. Functional characterization of *StCYP80B in vivo* and *in vitro*

To validate the catalytic function of *St*CYP80B, heterologous expressions of pESC-Leu-*StCYP80B*, pESC-Leu-*StCYP80B-StCPR1*, and pESC-Leu-*StCYP80B-StCPR2* vectors were detected independently in yeast (*S. cerevisiae)*. Yeast cells transformed with the pESC-Leu vector served as the control. Four racemic substrates, specifically *N*-methylcoclaurine, coclaurine, norcoclaurine, and armepavine, were individually introduced to the transgenic yeast cells. LC-MS/MS analysis (Fig. 5) demonstrated that *St*CYP80B

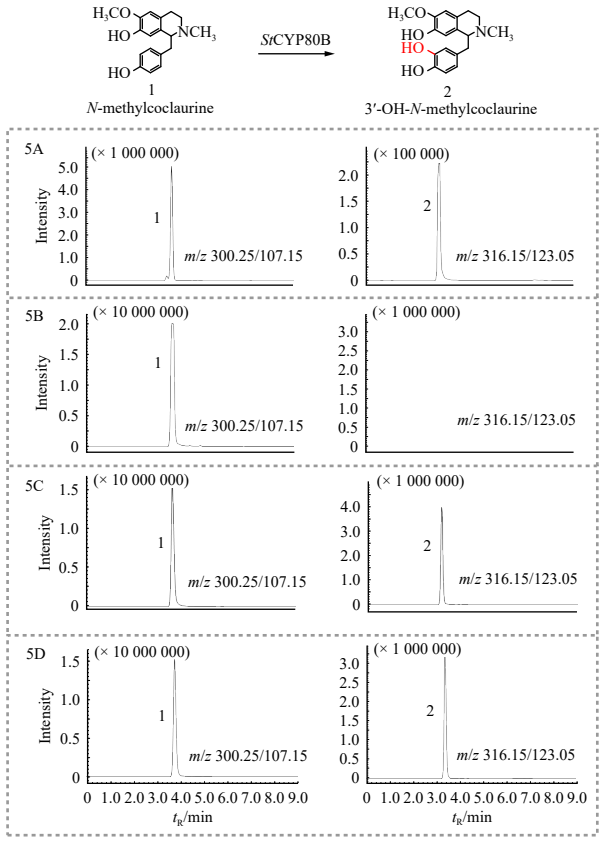

Fig. 5 LC-MS/MS analysis of *in-vivo St*CYP80B and *St*CPR1 reaction system catalyzing substrate *N*-methylcoclaurine. (A) Standards of *N*-methylcoclaurine and 3′-OH-*N*-methylcoclaurine; (B) Control reaction without *St*CYP80B and *St*CPRs; (C) *St*CYP80B-catalyzed reaction with *St*CPR1; (D) *St*CYP80B-catalyzed reaction without *St*CPRs. Peak 1: *N*-methylcoclaurine (*m/z* 300.25/107.15, t_R3.7 min); 2: 3′-OH-*N*-methylcoclaurine (*m/z* 316.15/123.05, t_R 3.2 min).

specifically catalyzed the conversion of (±)-*N*-methylcoclaurine (**1**, *m/z* 300.25/107.15) to its hydroxylation product (**2**, *m/z* 316.15/123.05). Likewise, *St*CYP80B distinctly transformed (±)-coclaurine (**3**, *m/z* 286.25/107.15) into its hydroxylation product (**4**, *m/z* 302.15/123.05), as illustrated in Fig. 6. Compounds **2** and **4** were identified as 3′-OH-*N*-methylcoclaurine and 3′-OH-coclaurine, respectively, through comparison with authentic standards. However, the addition of (±)-norcoclaurine and (±)-armepavine to the cells did not yield detectable corresponding hydroxylation products.

To further validate the functionality of *St*CYP80B, *in vitro* enzymatic assays were performed. Microsomal proteins were extracted from *St*CYP80B transgenic yeast cells co-expressing either with *St*CPR1 or *St*CPR2. Subsequently, (±)-*N*-methylcoclaurine and (±)-coclaurine were incubated with the microsomes, resulting in the production of their respective 3′-hydroxylation products (Supplementary Figs. S4 and S5). Compared to the previously reported wild-type CYP80Bs from other species, such as *E. californica* and *C. yanhusuo*, *St*CYP80B demonstrates a broader substrate selectivity. Earlier studies have indicated that the reported CYP80Bs require an *N*-methyl group for hydroxylase activity [8, 10]. The consistent results obtained from both the *in vivo* feeding assay and the *in vitro* enzyme assay provided conclusive evidence that *St*CYP80B was the first wide-type enzyme capable of catalyzing the conversion of both *N*-methylcoclaurine and coclaurine into their respective 3′-hydroxylated products. Virus-induced gene silencing (VIGS) in opium poppy plants implicated (*S*)-coclaurine as a key branch-point intermediate in the biosynthesis of *N*-demethylated alkaloids, such as papaverine [7]. The expanded substrate selectivity of *St*CYP80B suggests its pivotal role in the biosynthesis of downstream BIAs without *N*-methyl groups in *S. tetrandra* (Fig.1, NH pathway), such as norreticuline [16].

To evaluate the stereoselectivity of *St*CYP80B, we obtained optically pure (*R*)-coclaurine and (*S*)-coclaurine were obtained through chiral separation (Supplementary Figure S2), while (*R*)-*N*-methylcoclaurine was acquired from a commercial source. The *in vivo* catalytic experiment using these optically pure substrates (Figs. S6 and S7) revealed that supplementation of (*S*)-coclaurine to the yeast cells resulted in a significant production of 3′-OH-coclaurine. Conversely, supplementation with (*R*)-coclaurine or (*R*)-*N*-methylcoclaurine did not produce quantifiable 3′-hydroxylation products. These results demonstrate that *St*CYP80B exhibits a clear preference for the *S*-configuration. The observed stereoselectivity of *St*CYP80B is consistent with the characteristics of the known CYP80Bs [8, 10], which also require the *S*-configuration in the substrate for hydroxylase activity.

3.4. Enhanced catalytic activity of *StCYP80B* toward *(S)*-coclaurine through co-expression with *StCPRs*

The catalytic functions of most eukaryotic cytochrome P450 enzymes (CYP450s) necessitate the support of NADPH-cytochrome CPRs through a two-step, single-electron transfer process from NADPH to the prosthetic heme group of CYP450s. Research has demonstrated that the interactions between CYP450s and CPRs are complex and diverse, significantly impacting the production of metabolites [29].

Our comparative analysis of *St*CYP80B expression alone and in combination with *St*CPRs further elucidated the critical role of CPRs. *St*CYP80B, when expressed independently in transgenic yeast cells, demonstrated minimal catalytic activity towards(*S*)-coclaurine. Notably, co-expression of *St*CYP80B with either *St*CPR1 or *St*CPR2 resulted in a substantial increase in coclaurine hydroxylation activity, reaching levels approximately 100-fold higher than those observed without a redox partner (Fig. 7A). However, the hydroxylation activity of *St*CYP80B with either *St*CPR1 or *St*CPR2 towards *N*-methylcoclaurine

showed no significant difference compared to the expression of *St*CYP80B alone. Co-expression of CPRs from diverse sources with monooxygenases frequently alters enzyme activity and product profiles [35, 43-45], providing a method to optimize and modify CYP450 characteristics in the artificial biosynthesis of natural products. This study confirms that co-expression of *St*CYP80B with appropriate *St*CPRs effectively enhances *St* CYP80B activity on (*S*)-coclaurine, offering a potential strategy to exploit the capabilities of CYP450s.

3.5. Protein modeling, ligand docking, and key residue analysis of StCYP80B

The crystal structure analysis of plant CYP450s presents challenges due to their membrane localization, resulting in limited available crystal structures for these enzymes. To address this limitation, structure modeling and ligand docking provide valuable tools for examining the structure-function relationships of proteins [25, 46, 47]. A previous study on the homology model of *Ec*-CYP80B identified six contiguous amino acid chains (C1: 94 to 109, C2: 202 to 205, C3: 271 to 294, C4: 344 to 356, C5: 416 to 434, C6: 465 to 468) as key regions in the substrate binding pocket. Additionally, a mutant (L203S) of *Ec*CYP80B demonstrated significant activity towards the substrate coclaurine, enhancing norreticuline production in a norreticuline-producing yeast strain[11]. Recently, AlphaFold has revolutionized protein structure modeling [25]. To elucidate the coclaurine catalytic mechanism of *St*CYP80B, we developed a model using the non-homology-based modeling method —AlphaFold 3, and predicted the substrate binding pocket for coclaurine. Through analysis and comparison of the substrate binding pockets of *St*CYP80B and *Ec*CYP80B, focusing on the positions with amino acid variances between the two enzymes, five sites were identified as potentially influencing catalytic activity. Subsequently, site-directed mutagenesis was performed on *St*CYP80B, generating five *St*CYP80B variants with substituted amino acids (H205Y, I206L, Q208R, M212L, and A357P). Among the variants investigated, the H205Y variant of *St*CYP80B exhibited a significant decrease in hydroxylation activity —over 70-fold when co-expressed with *St*CPR1 or *St*CPR2, and 5-fold when expressed without *St*CPRs (Fig. 7A). The catalytic results of the four other mutations are presented in Supplementary Fig. S8. Molecular docking of the

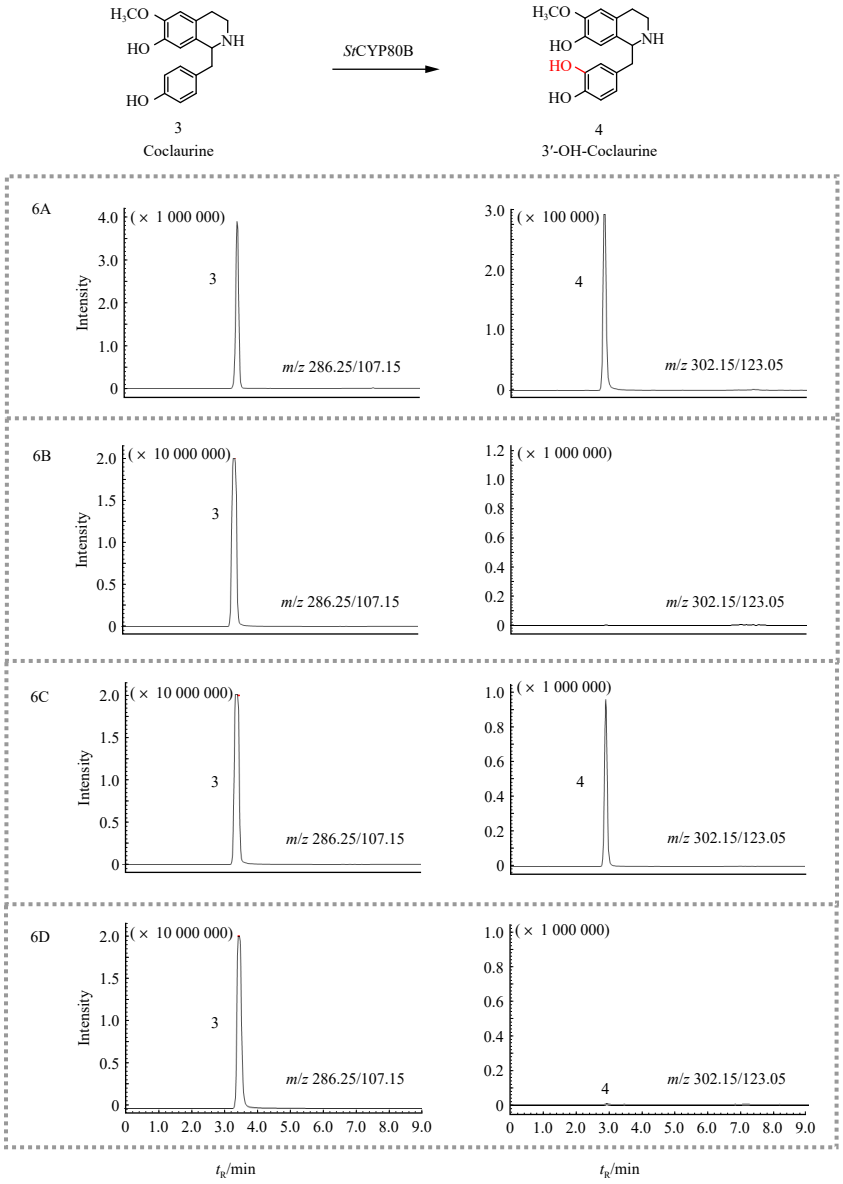

Fig. 6 LC-MS/MS analysis of *in-vivo St*CYP80B and *St*CPR1 reaction system catalyzing substrate coclaurine. (A) Standards of coclaurine and 3′-OH-coclaurine; (B) Control reaction without *St*CYP80B and *St*CPRs; (C) *St*CYP80B-catalyzed reaction with *St*CPR1; (D) *St*CYP80B-catalyzed reaction without *St*CPRs. Peak 3: coclaurine (*m/z* 286.25/107.15, t_R 3.3 min); 4: 3′-OH-coclaurine (*m/z* 302.15/123.05, t_R 2.8 min).

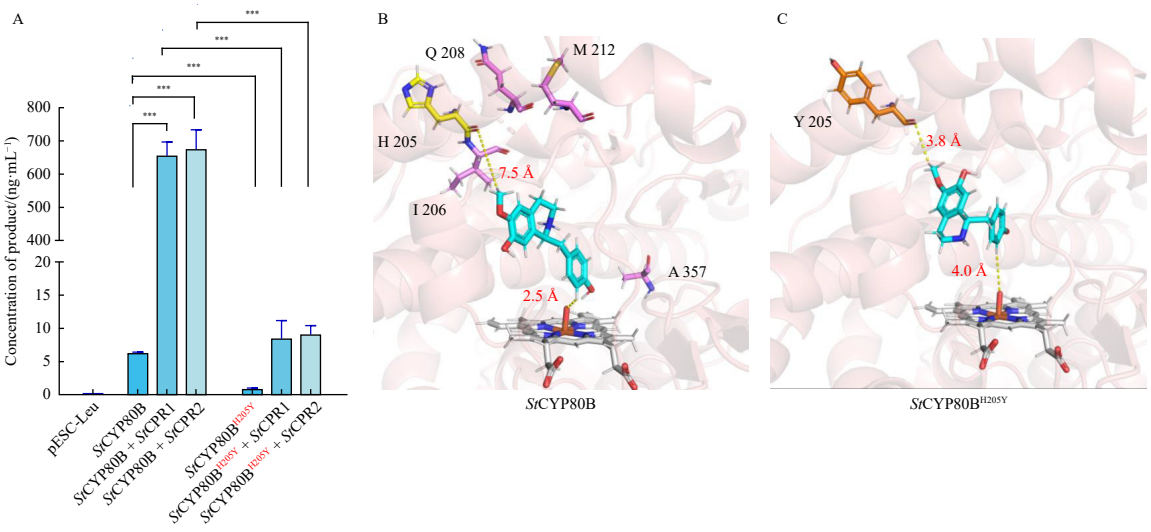

Fig. 7 Influence of co-expression with CPRs and mutation of crucial amino acid H205 on the hydroxylation function of CYP80B. (A) Concentration of (*S*)-3′-OH-coclaurine produced by pESC-Leu, *St*CYP80B with and without *St*CPRs, and a mutant *St*CYP80B^{H205Y} with and without *St*CPRs. Three biological duplications were performed for each enzyme reaction (*** $P < 0.001$). (B) Molecular docking of *St*CYP80B and (*S*)-coclaurine. (C) Molecular docking of *St*CYP80B^{H205Y} and (*S*)-coclaurine. The H205 residue of *St*CYP80B is highlighted in yellow, and the mutant Y205 residue is shown in orange. The four other residues I206, Q208, M212, and A357 are indicated in purple. (*S*)-coclaurine is shown in cyan, and heme is displayed in grey.

wide-type *St*CYP80B and the histidine-to-tyrosine mutant *St*CYP80B^{H205Y} with the substrate (*S*)-coclaurine (Figs. 7B and C) indicated a close distance (3.8 Å inFig. 7C) between the carbonyl group of tyrosine and the hydrogen atom of 6-methoxy on the substrate. This proximity potentially leads to hydrogen bond formation and an increased distance between H-3′ of (*S*)-coclaurine and Fe=O of heme (observed at 2.5 Å in Fig. 7B and 4.0 Å in-Fig. 7C). In conclusion, the residue H205 of *St*CYP80B plays a crucial role in its catalytic activity towards (*S*)-coclaurine.

3.6. Tissue-specific expression analysis

*St*CYP80B is a crucial enzyme involved in the biosynthesis pathway of BIAs. The enzymatic activity of *St*CYP80B towards specific substrates is influenced by the presence of *St*CPR1 and *St*CPR2. To examine the expression patterns of these genes, a qRT-PCR assay was conducted on six tissues of *S. tetrandra*: the main root, lateral root, periderm, and phloem of the main root, xylem of the main root, stem, and leaf. As illustrated in Fig.8, *StCYP80B* demonstrates relatively higher expression levels in the underground parts compared to the aerial parts. It also exhibits a significantly higher level in the outer part of the main root (including the periderm and phloem) than in the inner part (xylem). Previous research has shown that BIA metabolites primarily accumulate in the underground parts of *S. tetrandra*, particularly in the epidermis [21, 48, 49]. Consequently, the expression pattern of *StCYP80B* aligns with the distribution pattern of BIA metabolites.

However, the expression levels of the two *CPR* genes identified in *S. tetrandra* do not exhibit a clear correlation with BIA accumulation in roots. Notably, plants generally possess two types of *CPR* genes. One type is characterized by constitutive expression, while the expression of the other type can be induced by external stimuli such as wounding, light exposure, or MeJA treatment [41, 42, 50]. In the case of *S. tetrandra*, it is plausible that the two *StCPRs* are involved in a broad spectrum of oxidative reactions within the plant, rather than being exclusively associated with BIA biosynthesis. Consequently, their expression patterns may not consistently align with the BIA distribution.

4. Conclusions

In conclusion, this study successfully isolated and characterized a CYP80B gene (*StCYP80B*) and two CPR genes (*StCPR1* and *StCPR2*) from *S. tetrandra*. Through *in vivo* yeast feeding experiments and *in vitro* enzyme analyses, *St* CYP80B was confirmed to catalyze the 3'-hydroxylation of (*S*)-*N*-methylcoclaurine and (*S*)-coclaurine. Significantly, *St*CYP80B demonstrated broader substrate selectivity compared to the previously reported wild-type CYP80s, functioning without the requirement of an *N*-methyl group for hydroxylase activity. Moreover, *St*CYP80B exhibited a distinct preference for the (*S*)-configuration. Co-expression of *St*CYP80B with *St*CPRs notably enhanced the activity of *St*CYP80B on (*S*)-coclaurine. The substitution of the key residue H205 substantially influenced the catalytic activity of *St*CYP80B towards (*S*)-coclaurine. Furthermore, *St*CYP80B displayed tissue-specific expression patterns in plants. The identification of the wild-type enzyme, *St*CYP80B, corroborates the existence of the proposed *N*-desmethylated pathway within natural plant systems. This re-

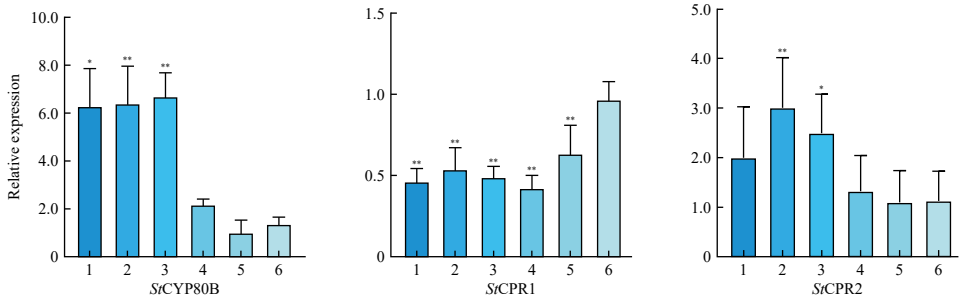

Fig. 8 Relative expression levels of *StCYP80B*, *StCPR1*, and *StCPR2* in six tissues of *S. tetrandra*. Group 1: main root; 2: lateral root; 3: periderm and phloem of main root; 4: xylem of main root; 5: stem, 6: leaf ($n = 3$, * $P < 0.05$, ** $P < 0.01$ versus the leaf group). The genes were analyzed by qRT-PCR with actin as a reference gene.

search advances our understanding of CYP80Bs, offering comprehensive insights into the biosynthetic pathway of BIAs.

Supplementary Information

Supplementary material related to this article can be requested by sending E-mail to the corresponding authors.

References

1 Wang M, Zhang XM, Fu X, et al. Alkaloids in genus *Stephania* (Menispermaceae): a comprehensive review of its ethnopharmacology, phytochemistry, pharmacology and toxicology. *J Ethnopharmacol*. 2022;293:115-248. https://doi.org/10.1016/j.jep.2022.115248.

2 Narcross L, Fossati E, Bourgeois L, et al. Microbial factories for the production of benzylisoquinoline alkaloids. *Trends Biotechnol*. 2016;34(3):228-241. https://doi.org/10.1016/j.tibtech.2015.12.005.

3 Lin Z, Hu ZW, Qu XD, et al. Advances and challenges in microbial production of benzylisoquinoline alkaloids. *Synth Biol J*. 2021;2(5):716-733. https://doi.org/10.12211/2096-8280.2021-058.

4 Samanani N, Facchini PJ. Isolation and partial characterization of norcoclaurine synthase, the first committed step in benzylisoquinoline alkaloid biosynthesis, from opium poppy. *Planta*. 2001;213(6):898-906. https://doi.org/10.1007/s004250100581.

5 Morishige T, Tsujita T, Yamada Y, et al. Molecular characterization of the *S*-adenosyl-L-methionine: 3'-hydroxy-*N*-methylcoclaurine 4'-*O*-methyltransferase involved in isoquinoline alkaloid biosynthesis in *Coptis japonica*. *J Biol Chem*. 2000;275(30):23398-23405. https://doi.org/10.1074/jbc.M002439200.

6 Choi KB, Morishige T, Shitan N, et al. Molecular cloning and characterization of coclaurine *N*-methyltransferase from cultured cells of *Coptis japonica*. *J Biol Chem*. 2002;277(1):830-835. https://doi.org/10.1074/jbc.M106405200.

7 Desgagné-Penix I, Facchini PJ. Systematic silencing of benzylisoquinoline alkaloid biosynthetic genes reveals the major route to papaverine in opium poppy. *J Plant*. 2012;72(2):331-344. https://doi.org/10.1111/j.1365-313X.2012.05084.x.

8 Pauli HH, Kutchan TM. Molecular cloning and functional heterologous expression of two alleles encoding (*S*)-*N*-methylcoclaurine 3'-hydroxylase (CYP80B1), a new methyl jasmonate-inducible cytochrome P-450-dependent mono-oxygenase of benzylisoquinoline alkaloid biosynthesis. *J Plant*. 1998;13(6):793-801. https://doi.org/10.1046/j.1365-313X.1998.00085.x.

9 Huang FC, Kutchan TM. Distribution of morphinan and benzo[*c*] phenanthridine alkaloid gene transcript accumulation in *Papaver somniferum*. *Phytochemistry*. 2000;53(5):555-564. https://doi.org/10.1016/S0031-9422(99)00600-7.

10 Liu XY, Bu JL, Ma Y, et al. Functional characterization of (*S*)-*N*-methylcoclaurine 3'-hydroxylase (NMCH) involved in the biosynthesis of benzylisoquinoline alkaloids in *Corydalis yanhusuo*. *Plant Physiol Biochem*. 2021;168:507-515. https://doi.org/10.1016/j.plaphy.2021.09.042.

11 Jamil OK, Cravens A, Payne JT, et al. Biosynthesis of tetrahydropapaverine and semisynthesis of papaverine in yeast. *Proc Natl Acad Sci USA*. 2022;119(33):e2205848119. https://doi.org/10.1073/pnas.2205848119.

12 National Pharmacopoeia Commission. Pharmacopoeia of the People's Republic of China. Vol. 1. Chinese Medical Science and Technology Press, Beijing, China, 2020: pp. 155-156.

13 Zhang YL, Qi DL, Gao YQ, et al. History of uses, phytochemistry, pharmacological activities, quality control and toxicity of the root of *Stephania tetrandra* S. Moore: a review. *J Ethnopharmacol*. 2020;260:112995. https://doi.org/10.1016/j.jep.2020.112995.

14 Jiang YP, Liu M, Liu HT, et al. A critical review: traditional uses, phytochemistry, pharmacology and toxicology of *Stephania tetrandra* S. Moore (Fen Fang Ji). *Phytochem Rev*. 2020;19:1-41. https://doi.org/10.1007/s11101-020-09673-w.

15 Chen JF, Zhao Q, Si DD, et al. Comprehensive profiling of *Stephania tetrandra* (Fangji) by stepwise DFI and NL-dependent structure annotation algorithm-based UHPLC-Q-TOF-MS and direct authentication by LMJ-HRMS. *J Pharm Biomed Anal*. 2020;185:113225. https://doi.org/10.1016/j.jpba.2020.113225.

16 Xue JY, Liu S, Kang Y, et al. An integrated strategy for characterization of chemical constituents in *Stephania tetrandra* using LC-QTOF-MS/MS and the target isolation of two new biflavonoids. *J Pharm Biomed Anal*. 2023;226:115247. https://doi.org/10.1016/j.jpba.2023.115247.

17 Kashiwada Y, Aoshima A, Ikeshiro Y, et al. Anti-HIV benzylisoquinoline alkaloids and flavonoids from the leaves of *Nelumbo nucifera*, and structure–activity correlations with related alkaloids. *Bioorg Med Chem*. 2005;13(2):443-448. https://doi.org/10.1016/j.bmc.2004.10.020.

18 Majrashi TA, Zulfiqar F, Chittiboyina AG, et al. Isoquinoline alkaloids from *Asimina triloba*. *Nat Prod Res*. 2019;33(19):2823-2829. https://doi.org/10.1080/14786419.2018.1504045.

19 Yang L, Zhu JM, Sun CH, et al. Biosynthesis of plant tetrahydroisoquinoline alkaloids through an imine reductase route. *Chem Sci*. 2020;11(2):364-371. https://doi.org/10.1039/C9SC03773J.

20 Jiang T, Liu ZZ, Yao YX. Research progress of detection methods for chemical components from *Nelumbinis Plumula*. *Chin Tradit Pat Med*. 2020;42(2):446-451. https://d.wanfangdata.com.cn/periodical/zhongcy202002032

21 Zhang YY, Kang Y, Xie H, et al. Comparative transcriptome analysis reveals candidate genes involved in Isoquinoline alkaloid biosynthesis in *Stephania tetrandra*. *Planta Med*. 2020;86(17):1258-1268. https://doi.org/10.1055/a-1209-3407.

22 Sievers F, Wilm A, Dineen D, et al. Fast, scalable generation of high-quality protein multiple sequence alignments using Clustal Omega. *Mol Syst Biol*. 2011;7:539. https://doi.org/10.1038/msb.2011.75.

23 Robert X, Gouet P. Deciphering key features in protein structures with the new ENDscript server. *Nucleic Acids Res*. 2014;42(W1):W320-324. https://doi.org/10.1093/nar/gku316.

24 Ikezawa N, Tanaka M, Nagayoshi M, et al. Molecular cloning and characterization of CYP719, a methylenedioxy bridge-forming enzyme that belongs to a novel P450 family, from cultured *Coptis japonica* cells. *J Biol Chem*. 2003;278(40):38557-38565. https://doi.org/10.1074/jbc.M302470200.

25 Abramson J., Adler J., Dunger J. et al. Accurate structure prediction of biomolecular interactions with AlphaFold 3. *Nature*. 2024;630:493-500. https://doi.org/10.1038/s41586-024-07487-w.

26 Livak KJ, Schmittgen TD. Analysis of relative gene expression data using real-time quantitative PCR and the $2^{-\Delta\Delta CT}$ method. *Methods*. 2001;25(4):402-408. https://doi.org/10.1006/meth.2001.1262.

27 Samanani N, Park S, Facchini PJ. Cell type-specific localization of transcripts encoding nine consecutive enzymes involved in protoberberine alkaloid biosynthesis. *Plant Cell*. 2005;17(3):915-926. https://doi.org/10.1105/tpc.104.028654.

28 Jensen K, Moller BL. Plant NADPH-cytochrome P450 oxidoreductases. *Phytochemistry*. 2010;71(2-3):132-141. https://doi.org/10.1016/j.phytochem.2009.10.017.

29 Parage C, Foureau E, Kellner F, et al. Class II cytochrome P450 reductase governs the biosynthesis of alkaloids. *Plant Physiol*. 2016;172(3):1563-1577. https://doi.org/10.1104/pp.16.00801.

30 Ro DK, Ehlting J, Douglas CJ. Cloning, functional expression, and subcellular localization of multiple NADPH-cytochrome P450 reductases from Hybrid Poplar. *Plant Physiol*. 2002;130(4):1837-1851. https://doi.org/10.1104/pp.008011.

31 Kraus PF, Kutchan TM. Molecular cloning and heterologous expression of a cDNA encoding berbamunine synthase, a C-O phenol-coupling cytochrome P450 from the higher plant *Berberis stolonifera*. *Proc Natl Acad Sci USA*. 1995;92(6):2071-2075. https://doi.org/10.1073/pnas.92.6.2071.

32 Ikezawa N, Iwasa K, Sato F. Molecular cloning and characterization of CYP80G2, a cytochrome P450 that catalyzes an intramolecular C-C phenol coupling of (*S*)-reticuline in magnoflorine biosynthesis, from cultured *Coptis japonica* cells. *J Biol Chem*. 2008;283(14):8810-8821. https://doi.org/10.1074/jbc.M705082200.

33 Dang TTT, Chen X, Facchini PJ. Acetylation serves as a protective group in noscapine biosynthesis in opium poppy. *Nat Chem Biol*. 2014;11:104-106. https://doi.org/10.1038/nchembio.1717.

34 Beaudoin GAW, Facchini PJ. Isolation and characterization of a cDNA encoding (*S*)-cis-N-methylstylopine 14-hydroxylase from opium poppy, a key enzyme in sanguinarine biosynthesis. *Biochem Biophys Res Commun*. 2013;431(3):597-603. https://doi.org/10.1016/j.bbrc.2012.12.129.

35 Gesell A, Rolf M, Ziegler J, et al. CYP719B1 is salutaridine synthase, the C-C phenol-coupling enzyme of morphine biosynthesis in opium poppy. *J Biol Chem*. 2009;284(36):24432-24442. https://doi.org/10.1074/jbc.M109.033373.

36 Olsen KM, Hehn A, Jugde H, et al. Identification and characterisation of CYP75A31, a new flavonoid 3'5'-hydroxylase, isolated from *Solanum lycopersicum*. *BMC Plant Biol*. 2010;10:21. https://doi.org/10.1186/1471-2229-10-21.

37 Kaltenbach M, Schroder G, Schmelzer E, et al. Flavonoid hydroxylase from *Catharanthus roseus*: cDNA, heterologous expression, enzyme properties and cell-type specific expression in plants. *Plant J*. 1999;19(2):183-193. https://doi.org/10.1046/j.1365-313X.1999.00524.x.

38 Seki H, Ohyama K, Sawai S, et al. Licorice beta-amyrin 11-oxidase, a cytochrome P450 with a key role in the biosynthesis of the triterpene sweetener glycyrrhizin. *Proc Natl Acad Sci U S A*. 2008;105(37):14204-14209. https://doi.org/10.1073/pnas.0803876105.

39 Mizutani M, Ward E, DiMaio J, et al. Molecular cloning and sequencing of a cDNA encoding mung bean cytochrome P450 ($P450_{C4H}$) possessing cinnamate 4-hydroxylase activity. *Biochem Biophys Res Commun*. 1993;190(3):875-880. https://doi.org/10.1006/bbrc.1993.1130.

40 Li SW, Shi RF, Leng Y. De novo characterization of the mung bean transcriptome and transcriptomic analysis of adventitious rooting in seedlings using RNA-Seq. *PLOS One*. 2015;10(7):e0132969. https://doi.org/

10.1371/journal.pone.0132969.
41 Mizutani M, Ohta D. Two isoforms of NADPH: cytochrome P450 reductase in *Arabidopsis thaliana*: gene structure, heterologous expression in insect cells, and differential regulation. *Plant Physio*. 1998;116(1):357-367. https://doi.org/10.1104/pp.116.1.357.
42 Lin HX, Wang J, Qi MD, et al. Molecular cloning and functional characterization of multiple NADPH-cytochrome P450 reductases from *Andrographis paniculata*. *Int J Biol Macromol*. 2017;102:208-217. https://doi.org/10.1016/j.ijbiomac.2017.04.029.
43 Rosco A, Pauli HH, Priesner W, et al. Cloning and heterologous expression of NADPH-cytochrome P450 reductases from the Papaveraceae. *Arch Biochem Biophys*. 1998;348(2):369-377. https://doi.org/10.1006/abbi.1997.0374.
44 Payne JT, Valentic TR, Smolke CD. Complete biosynthesis of the bisbenzylisoquinoline alkaloids guattegaumerine and berbamunine in yeast. *Proc Natl Acad Sci USA*. 2021;118(51):e2112520118. https://doi.org/10.1073/pnas.2112520118.
45 Guo J, Zhou YJ, Hillwig ML, et al. CYP76AH1 catalyzes turnover of miltiradiene in tanshinones biosynthesis and enables heterologous production of ferruginol in yeasts. *Proc Natl Acad Sci USA*. 2013;110(29):12108-12113. https://doi.org/10.1073/pnas.1218061110.
46 Vazquez-Albacete D, Montefiori M, Kol S, et al. The CYP79A1 catalyzed conversion of tyrosine to (*E*)-*p*-hydroxyphenylacetaldoxime unravelled using an improved method for homology modeling. *Phytochemistry*. 2017;135:8-17. https://doi.org/10.1016/j.phytochem.2016.11.013.
47 Wang H, Wang Q, Liu YQ, et al. PCPD: plant cytochrome P450 database and web-based tools for structural construction and ligand docking. *Synth Syst Biotechnol*. 2021;6(2):102-109. https://doi.org/10.1016/j.synbio.2021.04.004.
48 Li KL, Chen XF, Zhang JB, et al. Transcriptome analysis of *Stephania tetrandra* and characterization of Norcoclaurine-6-*O*-Methyltransferase involved in benzylisoquinoline alkaloid biosynthesis. *Front Plant Sci*. 2022;13:874583. https://doi.org/10.3389/fpls.2022.874583.
49 Li QS, Bu JL, Ma Y, et al. Characterization of *O*-methyltransferases involved in the biosynthesis of tetrandrine in *Stephania tetrandra*. *J Plant Physiol*. 2020;250:153181. https://doi.org/10.1016/j.jplph.2020.153181.
50 Yang CQ, Lu S, Mao YB, et al. Characterization of two NADPH: cytochrome P450 reductases from cotton (*Gossypium hirsutum*). *Phytochemistry*. 2010;71(1):27-35. https://doi.org/10.1016/j.phytochem.2009.09.026.